Inorganic Chemistry

Article

pubs.acs.org/IC

Crystal Structure and Physical Properties of the New One-Dimensional Metal $Ba_2Cu_{7-x}Te_6$

Bryan A. Kuropatwa, Abdeljalil Assoud, and Holger Kleinke*

Department of Chemistry and Waterloo Institute of Nanotechnology, University of Waterloo, Waterloo, Ontario, Canada N2L 3G1

Supporting Information

ABSTRACT: The telluride $Ba_2Cu_{7-x}Te_6$ was synthesized from the elements in stoichiometric ratios, heated to 1073 K, followed by slow cooling to 873 K over 120 h. $Ba_2Cu_{7-x}Te_6$ crystallizes in space group $P2_1/m$ with lattice dimensions of a = 6.8591(7) Å, b = 12.1439(12) Å, c = 9.0198(9) Å, β = 110.7509(14)°, V = 702.58(12) Å^3, and Z = 2. The structure is comprised of Cu atoms forming a six-membered ring and triangles, interconnected to an infinite ribbon of Cu atoms. The ribbons are connected to each other via Cu−Te bonds to yield a three-dimensional structure, wherein each Cu atom is tetrahedrally coordinated by four Te atoms. A special feature of this telluride is the occurrence of a quasi-linear Te atom chain, which causes one-dimensional metallic properties, in accordance with electronic structure calculations and property measurements.

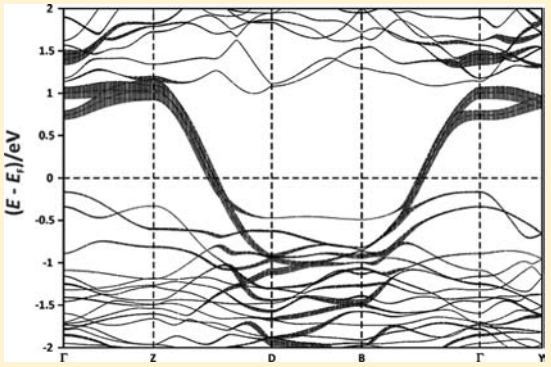

INTRODUCTION

Chalcogenides and polychalcogenides attract the attention of solid-state chemists, researchers, engineers, and materials scientists alike. Their practical semiconducting-based applications including electronics,[1] rechargeable batteries,[2] data storage,[3−5] and thermoelectric energy conversion[6−8] give chalcogenides a functional place in today's society. The thermoelectric efficiency depends on the thermoelectric figure-of-merit, ZT, with higher ZT values translating into higher efficiency. ZT is defined as $ZT = TS^2\sigma\kappa^{-1}$, with S = Seebeck coefficient, σ = electrical conductivity, and κ = thermal conductivity.[9] Therefore, the desired properties are high Seebeck coefficient and high electrical conductivity combined with low thermal conductivity, which is best achieved in narrow-gap semiconductors comprising heavy elements, such as in various antimonides[10−13] and tellurides.[14,15]

One of the systems under investigation for its thermoelectric properties is the Ba−Cu−Te system since 2001, beginning with $BaCu_2Te_2$,[16] and the quaternary tellurides $A_2BaCu_8Te_{10}$ (A = K, Rb, Cs).[17] Subsequently, we found three new ternary tellurides in this system, namely, $Ba_3Cu_{14-x}Te_{12}$,[18] $Ba_{6.76}Cu_{2.42}Te_{14}$,[19] and $Ba_2Cu_{4-x}Te_5$,[20] as well as several new, different quaternary sulfide−tellurides and selenide−tellurides: $Ba_2Cu_{6-x}STe_4$ and $Ba_2Cu_{6-x}Se_yTe_{5-y}$,[21] $BaCu_{6-x}STe_6$ and $BaCu_{6-x}Se_{1-y}Te_{6+y}$,[22] $Ba_2Cu_{4-x}Se_yTe_{5-y}$,[20] and $BaCu_{17-x}Se_{11-x}Te_y$.[23] All of these were characterized as Cu-deficient, and thus p-type semiconductors, with only one exception thus far, namely, the metallic sulfide−telluride $BaCu_{17-x}S_{11.5-y}Te_y$.[24] Because a high Ba:Cu ratio proved to be disadvantageous for thermoelectric properties (because of low electrical conductivity),[25] we have increasingly concentrated on smaller Ba:Cu ratios, along with an excess of tellurium, in order to obtain polytellurides, expected to cause the desired small band gaps.[26,27] During this process, we discovered the new telluride $Ba_2Cu_{7-x}Te_6$ with significant Te−Te interactions, which is introduced with this contribution.

EXPERIMENTAL SECTION

Syntheses. All reactions commenced from the elements (Ba, 99%, pieces, Aldrich; Cu, 99.5%, powder −150 mesh, Alfa Aesar; Te, 99.999%, ingot, Aldrich), with sample masses of approximately 600 mg. The elements were stored and handled in a glovebox filled with argon. Within, the elements were placed into glassy carbon crucibles inside silica tubes, which were subsequently sealed under vacuum (10^{-3} mbar). The tubes were then heated in a resistance furnace at 1073 K for 6 h. Thereafter, the furnace was slowly cooled to 923 K and left for a period of 60 h to allow for homogenization. Lastly, the furnace was switched off, prompting fast cooling. Investigations on the phase range of $Ba_2Cu_{7-x}Te_6$ were carried out with $0 \le x \le 1$ in increments of 0.2. Therein, the sample with x = 0.4 was found to be a pure phase, and the samples with x = 0.2 and 0.6 contained less than 5% side products, hinting toward the existence of a rather small phase range.

Analyses. The sample of nominal composition $Ba_2Cu_{6.6}Te_6$ was analyzed via energy-dispersive analysis of X-rays (EDAX) using an electron microscope (LEO 1530) with an additional EDX device (EDAX Pegasus 1200). The scans were performed with an acceleration voltage of 20 kV under a high dynamic vacuum. No heteroelements were detected during the examination. The obtained Ba:Cu:Te ratios were very homogeneous, yielding 14:45:41 atomic %, as averaged over six crystals, compared to the nominal 13.7:45.2:41.1.

Differential scanning calorimetry (DSC) equipped with thermogravimetry (TG) on a NETZSCH STA 409PC Luxx instrument was also utilized to study the thermal stability of $Ba_2Cu_{6.6}Te_6$. The compound was heated from room temperature to 1123 K under argon

Received: February 1, 2012
Published: April 18, 2012

   dx.doi.org/10.1021/ic300239c | *Inorg. Chem.* 2012, 51, 5299−5304

flow against a sapphire reference. Upon heating at a rate of 20 K min^{-1}, the experiment showed a single endothermic peak around 1000 K corresponding to the melting point; upon cooling at a rate of 20 K min^{-1}, the opposite exothermic crystallization peak was found around 900 K; throughout the measurement, thermogravimetry data remained stable between 99% and 98% of the initial starting mass. When this experiment was repeated with a rate of 20 K min^{-1}, these peaks occurred at 982 and 959 K, respectively. No phase changes or decompositions were observed in the aforementioned range (see the Supporting Information).

Structure Determination. A platelike single crystal of $Ba_2Cu_{7-x}Te_6$ was selected for data collection using a SMART Apex CCD with graphite-monochromatized Mo Kα_1 radiation (Bruker). Two sets of 606 frames were collected with an exposure time of 40 s $frame^{-1}$. The data were corrected for Lorentz and polarization effects. Absorption corrections were based on fitting a function to the empirical transmission surface as sampled by multiple equivalent measurements using the *SADABS* part of the *APEX II* package because there were no faces for indexation. Using *RLATT*, incorporated within the *APEX II* package, revealed that the crystal was a twin, and the twin reflections in the P4P list were separated using the *cell_now* program and gave the same cell for both components. The second individual is related to the first by a 180° rotation, $a_2 = -a_1$, $b_2 = -b_1$, and $c_2 = a_1 + c_1$. The integration and subsequent data reduction of both components was carried out using the *APEX II* package.[28]

The structure solution and refinements were performed with the *SHELXTL* program package,[29] and X-ray spectroscopy found two Ba (2e positions), four Cu (three on 4f and one on 2e), and four Te (two on 4f and two on 2e). As is often observed in copper chalcogenides, not all Cu sites were fully occupied: minor albeit significant deficiencies were found for Cu2, Cu3, and Cu4 of 2−12%, while the Cu1 occupancy was refined to 100% within 2 standard deviations [99.1(6)%]. Allowing for these deficiencies, the refinement's residuals of R1 = 0.0492 and wR2 = 0.1289 improved to 0.0473 and 0.1216, respectively. Ultimately, the formula was refined to $Ba_2Cu_{6.64(4)}Te_6$. Attempts to grow better single crystals using different heating conditions and different fluxes did not lead to any noticeable improvements, and the crystals were always twinned. Crystallographic data for $Ba_2Cu_{6.6}Te_6$ are given in Table 1.

Table 1. Crystallographic Data for $Ba_2Cu_{6.64(4)}Te_6$

refined formula	$Ba_2Cu_{6.64(4)}Te_6$
fw [g mol^{-1}]	1462.2
T of measurement [K]	298(2)
λ [Å]	0.71073
space group	$P2_1/m$
a [Å]	6.8591(7)
b [Å]	12.1439(12)
c [Å]	9.0198(9)
β	110.7509(14)
V [Å^3]	702.58(12)
Z	2
μ [mm^{-1}]	27.51
ρ_{calcd} [g cm^{-3}]	6.91
$R(F_o)^a/R_w(F_o^2)^b$	0.0573/0.1220

$^aR(F_o) = \sum||F_o| - |F_c||/\sum|F_o|$. $^bR_w(F_o^2) = [\sum[w(F_o^2 - F_c^2)^2]/\sum[w(F_o^2)^2]]^{1/2}$.

Calculation of the Electronic Structure. We utilized the linear muffin tin orbital (LMTO) method with the atomic sphere approximation for the electronic structure calculations.[30,31] Therein, density functional theory is applied with the local density approximation to treat correlation effects.[32] The following wave functions were used: for Ba, 6s, 6p (downfolded[33]), 5d, and 4f; for Cu, 4s, 4p, and 3d; for S, 3s, 3p, and 3d (downfolded); and for Te, 5s, 5p, 5d, and 4f (the latter two downfolded).

The full $Ba_2Cu_7Te_6$ model was calculated in $P2_1/m$, with the unit cell parameters pertaining to the crystal structure analyzed herein and all Cu sites fully occupied ($x = 0$). Removal of one Cu4 atom to yield $Ba_2Cu_{6.5}Te_6$ generates space group $P1$ ($x = 0.5$) and a 75% occupancy of Cu4, compared to the refined 88%. (Removing one Cu2 atom, for example, gave qualitatively the same electronic structure but is a less realistic model because then the Cu2 occupancy would be only 50%, while the refined value was 92%.) The eigenvalue problems were solved on the basis of 798 and 288 irreproducible k points, respectively. Points were chosen with an improved tetrahedron method.[34] To better understand the bonding in the structure, crystal orbital Hamiltonian populations (COHPs)[35,36] were calculated for the $x = 0$ case for all Cu−Cu interactions <3 Å, for the Te−Te contacts <3.6 Å, and for the Cu−Te contacts <2.8 Å.

Physical Property Measurements. A cold-pressed bar of dimensions 6 × 1 × 1 mm^3 of a $Ba_2Cu_{6.6}Te_6$ sample was used for the Seebeck coefficient (S) and electrical conductivity (σ) measurements. S and σ were simultaneously measured on a commercial ULVAC-RIKO ZEM-3 instrument from room temperature up to 725 K, with a thermocouple probe separation of approximately 3 mm. The electrical resistance (R) was determined via the four-point method and the Seebeck coefficient via $S = \Delta V/\Delta T$. The achieved density was around 85% of the theoretical maximum determined via the single-crystal structure study. The resistance (R) was calculated from the voltage drop ΔV using Ohm's law, i.e., $R = \Delta V/I$ with I = current. σ was calculated after measuring the lengths between the contacts, $L = 3$ mm, according to $\sigma = L/AR$ with the area $A = 1 \times 1$ mm^2.

RESULTS AND DISCUSSION

Crystal Structure. The new ternary telluride $Ba_2Cu_{6.6}Te_6$ crystallizes in a new structure type in the space group $P2_1/m$. The unit cell (Figure 1) contains two crystallographically

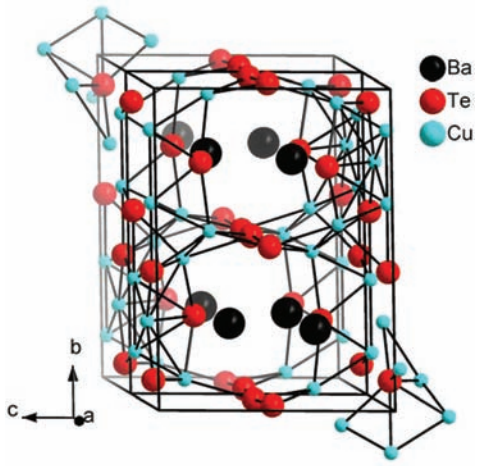

Figure 1. Crystal structure of $Ba_2Cu_{7-x}Te_6$. Ba−Te bonds are omitted for clarity.

independent Ba atoms (Ba1 and Ba2), both located on Wyckoff position 2e, and four Cu atoms (Cu1, Cu2, Cu3, and Cu4) located on Wyckoff positions 4f, 2e, 4f, and 4f with site deficiencies of 0%, 8%, 2%, and 12%, respectively. The four Te atoms (Te1, Te2, Te3, and Te4) occupy the positions 2e, 2e, 4f, and 4f, respectively (Table 2). The refined formula is $Ba_2Cu_{6.64(4)}Te_6$.

Both Ba atoms are centered in a tricapped trigonal prism, with Ba−Te bonds in the range between 3.45 and 3.9 Å (Table 3), similar to those found in many ternary Ba/Cu/Te compounds such $BaCu_2Te_2$ (3.40−3.61 Å),[16] $Ba_2Cu_{4-x}Te_5$ (3.44−4.02 Å),[20] and $Ba_3Cu_{14-x}Te_{12}$ (3.47−3.83 Å)[18] and in the binary tellurides BaTe (3.50 Å),[37] $BaTe_2$ (3.57 Å),[38] and

dx.doi.org/10.1021/ic300239c | Inorg. Chem. 2012, 51, 5299−5304

Table 2. Atomic Coordinates, Equivalent Isotropic Displacement Parameters, and Occupancy Factors of $Ba_2Cu_{7-x}Te_6$

atom	site	x	y	z	U_{eq}/Å^2	occ.
Ba1	2e	0.59291(13)	$^1/_4$	0.64891(10)	0.0147(2)	1
Ba2	2e	0.93065(14)	$^1/_4$	0.32531(11)	0.0184(2)	1
Cu1	4f	0.1200(2)	0.13572(12)	0.99328(18)	0.0217(3)	1
Cu2	2e	0.4853(3)	$^1/_4$	0.9847(2)	0.0193(7)	0.921(9)
Cu3	4f	0.3297(2)	0.06097(12)	0.81129(18)	0.0213(5)	0.978(7)
Cu4	4f	0.3728(3)	0.03567(15)	0.2693(2)	0.0234(5)	0.881(7)
Te1	2e	0.12575(14)	$^1/_4$	0.74233(11)	0.0116(2)	1
Te2	2e	0.38038(14)	$^1/_4$	0.23640(11)	0.0131(2)	1
Te3	4f	0.25259(9)	0.58055(5)	0.00821(7)	0.01209(18)	1
Te4	4f	0.24466(13)	0.50397(7)	0.50881(8)	0.0209(2)	1

Table 3. Selected Interatomic Distances [Å] of $Ba_2Cu_{7-x}Te_6$

Ba1	Te1	1×	3.4475(13)	Cu4	Te3	1×	2.617(2)
	Te2	1×	3.4822(13)		Te2	1×	2.6223(18)
	Te3	2×	3.551(1)		Te4	1×	2.649(2)
	Te1	1×	3.5904(13)		Te4	1×	2.705(2)
	Te4	2×	3.649(1)				
	Te4	1×	3.831(1)				
				Cu1	Cu3	1×	2.695(2)
					Cu4	1×	2.761(2)
Ba2	Te2	1×	3.451(1)		Cu1	1×	2.776(3)
	Te3	2×	3.489(1)		Cu2	1×	2.890(2)
	Te1	1×	3.517(1)				
	Te2	1×	3.570(1)	Cu2	Cu3	2×	2.770(2)
	Te4	2×	3.7263(11)		Cu1	2×	2.890(2)
	Te4	2×	3.790(1)				
Cu1	Te3	1×	2.638(1)	Cu3	Cu4	1×	2.668(2)
	Te1	1×	2.667(2)		Cu1	1×	2.695(2)
	Te2	1×	2.674(2)		Cu2	1×	2.770(2)
	Te3	1×	2.767(2)				
				Cu4	Cu3	1×	2.668(2)
					Cu1	1×	2.761(2)
Cu2	Te2	1×	2.613(2)				
	Te1	1×	2.654(2)	Te4	Te4	1×	3.305(2)
	Te3	2×	2.7178(14)		Te4	1×	3.564(2)
Cu3	Te1	1×	2.6454(16)				
	Te3	1×	2.6547(16)				
	Te4	1×	2.6978(17)				
	Te3	1×	2.759(2)				

$BaTe_3$ (3.59 and 3.63 Å).[39] The $[BaTe_9]$ polyhedra share common faces, edges, and corners to form a three-dimensional network.

The Cu atoms are in tetrahedral coordination, with Cu−Te bonds ranging from 2.62 and 2.77 Å similar to those found in many ternary Ba/Cu/Te compounds, including in $BaCu_2Te_2$ (2.60−2.78 Å).[16] The $[CuTe_4]$ tetrahedra are distorted, with bond angles ranging from 84° to 120°. The $[Cu3Te_4]$ and $[Cu4Te_4]$ tetrahedra share common edges to form an eight-membered ring $[Cu_4Te_4]$. $[Cu1Te_4]$ tetrahedra share common edges with each other and common corners with the $[Cu2Te_4]$, $[Cu3Te_4]$, and $[Cu4Te_4]$ tetrahedra. The $[Cu4Te_4]$ tetrahedra form layers along the c axis, and these layers are connected to each other via the Te3 atoms. Ba2 atoms fill the space between the layers, and Ba1 is located in the center of the eight-membered ring $[Cu_4Te_4]$.

The Cu−Cu bonds are in the range between 2.67 and 2.89 Å. Similar Cu−Cu bonds were reported in numerous other heavy chalcogenides,[40] including $Ba_3Cu_{14-x}Te_{12}$.[18] The bonding character of these formally closed-shell (d^{10}−d^{10}) interactions is a consequence of the hybridization of the filled d states with the nominally empty, energetically higher-lying s and p orbitals.[41−43] Cu1 and Cu2 are coordinated to four Cu neighbors, Cu3 is coordinated to three Cu neighbors, and Cu4 has only two Cu neighbors. Cu1, Cu3, and Cu4 form an almost planar six-membered ring, which is connected to the next one via Cu2 atoms and Cu1−Cu1 bonds, ultimately fused into an infinite ribbon along the b axis (Figure 2). The triangles, each formed by one Cu2 and two Cu1, are almost isosceles.

With Ba in the 2+ oxidation state and Cu in the 1+ oxidation state, not all Te atoms of $Ba_2Cu_{6.6}Te_6$ can attain the 2− state ($2 \times 2 + 6.6 \times 1 = 10.6 < 12 = 6 \times 2$). While Te1, Te2, and Te3 are not bonded to each other and are thus in the 2− oxidation state, the Te4 atoms form an infinite distorted pseudolinear chain with alternating Te−Te distances of 3.30 and 3.56 Å with a bond angle of 174° (Figure 3). A similar Te chain but with shorter Te−Te contacts and with split sites was found in $Ba_2Cu_{4-x}Te_5$, with the shorter distances being around 3.0 Å.[20]

dx.doi.org/10.1021/ic300239c | Inorg. Chem. 2012, 51, 5299−5304

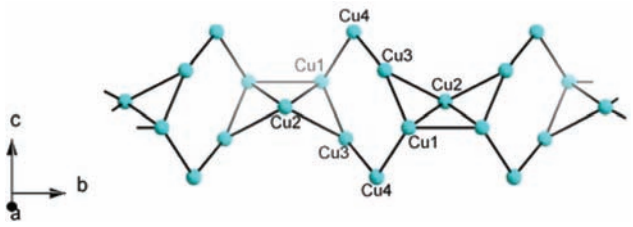

Figure 2. Infinite Cu ribbon in $Ba_2Cu_{7-x}Te_6$.

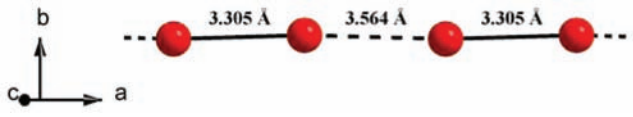

Figure 3. Infinite Te chain in $Ba_2Cu_{7-x}Te_6$.

The occurrence of a topologically equivalent Sb atom chain in $Zn_{4-\delta}Sb_3$[44] was speculated to be partially responsible for its extraordinarily low thermal conductivity (along with the complex structure and the multitude of different Zn-deficient sites[45]) caused by experimentally found "dumbbell rattling".[46]

The 3.3 Å distance of $Ba_2Cu_{6.6}Te_6$ is much longer than a Te−Te single bond of approximately 2.7−2.8 Å as is typically found in $[Te_2]^{2-}$ dumbbells, e.g., in $[N(CH_3)_4]_2Te_2$ (d_{Te-Te} = 2.74 Å)[47] and $[Na(CH_3OH)_3]_2Te_2$.[48] On the other hand, interlayer Te−Te distances <3.8 Å in layered transition-metal tellurides, such as 3.78 Å in $TiTe_2$, can have bonding character and be thus responsible for the metallic character of $TiTe_2$ because of the partially empty Te 5p states.[49]

Electronic Structure. The density of states, DOS, of both models, $Ba_2Cu_7Te_6$ and $Ba_2Cu_{6.5}Te_6$, exhibit a few numbers of states at the Fermi level, E_F (Figure 4). Examining the

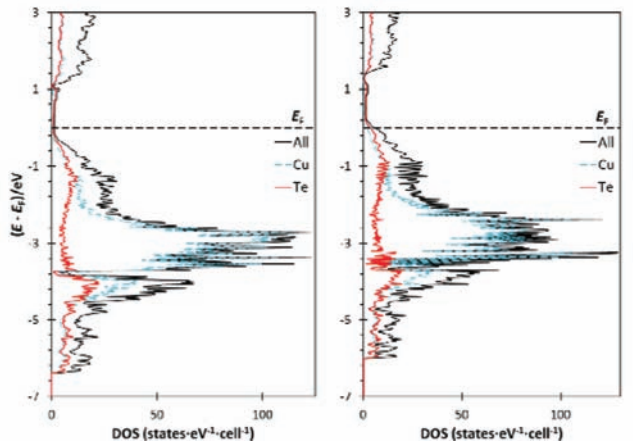

Figure 4. DOS of $Ba_2Cu_{7-x}Te_6$. Left: x = 0, $P2_1/m$. Right: x = 0.5, $P1$.

elemental contributions to the DOS, the energy levels below the Fermi level are predominantly Cu 3d states and Te 5p states. The most significant change to the DOS by going from $Ba_2Cu_7Te_6$ to $Ba_2Cu_{6.5}Te_6$ is the lowering of the Fermi level into a region with more filled Cu 3d states.

Analyzing the band structure is instructive in order to investigate the significance of the small numbers of states occurring at E_F. Therefore, fat-band[50] calculations were performed for the $Ba_2Cu_7Te_6$ model (Figure 5). The small DOS at E_F is evidently a consequence of two bands crossing the Fermi level parallel to a^* (Z-D and B-Γ), while no crossings

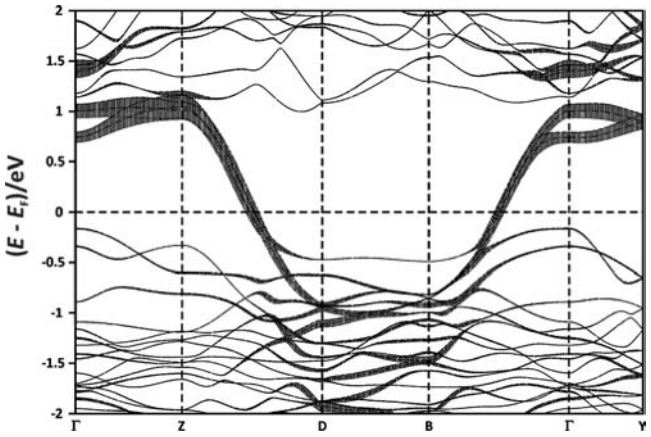

Figure 5. Band structure of $Ba_2Cu_7Te_6$ with highlighted Te4 p_x interactions via a fat-band representation. Fractional coordinates of the special points with respect to the reciprocal unit cell: Γ, (0, 0, 0); Z, (0, 0, $^1/_2$); D, ($^1/_2$, 0, $^1/_2$); B, ($^1/_2$, 0, 0); Y, (0, $^1/_2$, 0).

occur along any other direction, suggesting one-dimensional metallic behavior. These at E_F rather steep bands have a bandwidth of about 1.8 eV, and the primary contributions to these bands are from the Te4 p_x orbitals, with minor contributions from the Te4 p_z orbitals. This corresponds to the direction of the one-dimensional Te atom chains running along the a axis in the crystal structure. With the crystal structure solved for $Ba_2Cu_{6.6}Te_6$, it should also be noted that the Fermi level in this diagram would be slightly lower.

COHPs were calculated for Cu−Cu and Te−Te interactions of the model $Ba_2Cu_7Te_6$ (Figure 6). All Cu−Cu bonds

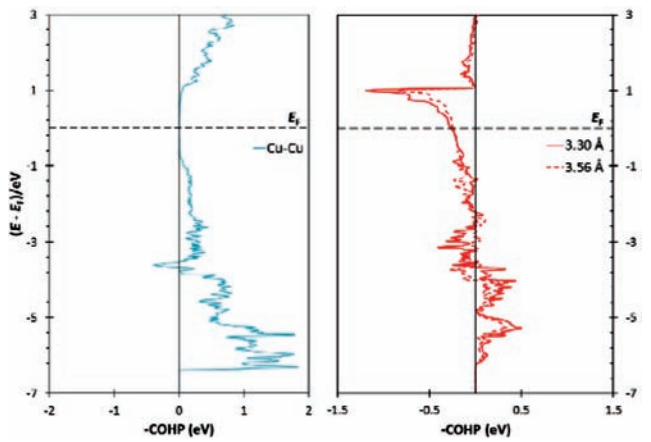

Figure 6. COHP curves of $Ba_2Cu_7Te_6$: left, Cu−Cu interactions; right, Te−Te interactions.

(between 2.69 and 2.89 Å) below the Fermi level have bonding character. While there are no Cu−Cu interactions near the Fermi level, the Cu−Cu states above 1 eV have bonding character as well, like many other compounds we studied in the Ba/Cu/Te system.[18,20,23] Its integrated COHP values (ICOHPs)[36] range from −0.30 to −0.52 eV per bond. Conversely, the Te−Te interactions, separated into 3.30 and 3.56 Å, do not show a strongly bonding character; the ICOHP at the Fermi level indicates that the 3.30 Å interaction is in total of a weakly bonding nature (ICOHP = −0.19 eV), while the 3.56 Å interaction is weakly antibonding (ICOHP = +0.06 eV). As in the case of $TiTe_2$, empty (antibonding) states exist in the

dx.doi.org/10.1021/ic300239c | Inorg. Chem. 2012, 51, 5299−5304

Te 5p band, as is evident from these COHP curves. The strongly antibonding character of both Te−Te interactions around the Fermi level combined with the Te4 chain running along the *a* axis is responsible for the steep character of the Te4 p_x-based bands.

Finally, the Cu−Te interactions are much stronger than the homonuclear ones and have only bonding states filled between −7 eV and E_F. A band gap separates the bonding from the antibonding states (see the Supporting Information).

Physical Properties. In order to determine its suitability for the thermoelectric energy conversion as well as to verify the results of the band structure calculation, physical properties were measured for a polycrystalline bulk sample with nominal composition $Ba_2Cu_{6.6}Te_6$ up to 725 K (Figure 7) because no large single crystals could be grown. The previously studied tellurides exhibit room temperature values of $S = 88\ \mu V\ K^{-1}$ and $\sigma = 126\ \Omega^{-1}\ cm^{-1}$ in the case of $BaCu_2Te_2$[16] and $S = 30\ \mu V\ K^{-1}$ and $\sigma = 190\ \Omega^{-1}\ cm^{-1}$ in the case of $Ba_3Cu_{13.88}Te_{12}$.[18] Seebeck coefficient values of $Ba_2Cu_{6.6}Te_6$ fell between +50 and +100 $\mu V\ K^{-1}$ for the full range of the measurement, showing a small but steady rise. The electrical conductivity was also reasonably steady with values falling from 180 $\Omega^{-1}\ cm^{-1}$ at 297 K to 167 $\Omega^{-1}\ cm^{-1}$ at 725 K, displaying a decreasing slope overall for the full measurement range. The values are thus intermediate between those of $BaCu_2Te_2$ and $Ba_3Cu_{13.88}Te_{12}$. Both physical property measurements are to be expected based on the aforementioned calculations; the band structure calculation predicts the compound's one-dimensional metal-like behavior such as a gradually decreasing electrical conductivity with increasing temperature and intermediate Seebeck coefficient. The resulting power factor shows a shape very similar to the Seebeck coefficient with a room temperature value of 0.43 $\mu W\ cm^{-1}\ K^{-2}$, which reached 1.45 $\mu W\ cm^{-1}\ K^{-2}$ at 725 K.

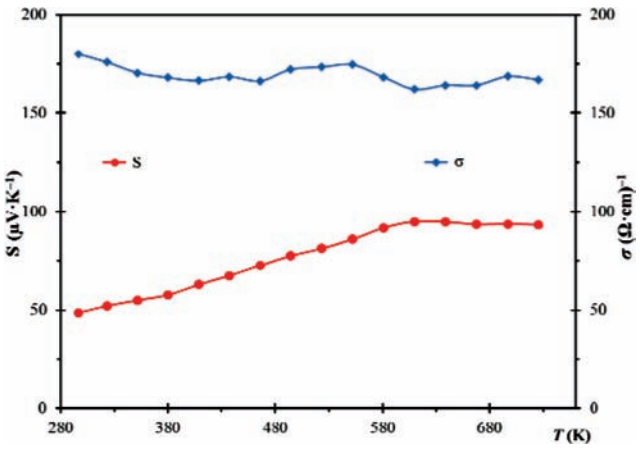

Figure 7. Seebeck coefficient (circles) and electrical conductivity (diamonds) of $Ba_2Cu_{6.6}Te_6$.

The metallic character, even though persistent in only one direction, stands against using this telluride in the thermoelectric energy conversion, unless one succeeds in preparing a device wherein the metallic direction is exclusively perpendicular to the carrier transport direction or one produces a more significant distortion into the Te chain, leading to a band-gap formation. While the latter occurs readily in the form of a Peierls distortion[51] in many one-dimensional materials, such as in the Te chain of $RbUSb_{0.33}Te_6$,[52] this case already displays a distorted chain, making a further introduction of a gap-opening distortion highly unlikely.

CONCLUSIONS

The new $Ba_2Cu_{7-x}Te_6$ telluride was discovered and characterized. Its crystal structure, determined by an X-ray structure determination, is of a new structure type with infinite zigzag chains of Cu_8 clusters and infinite distorted pseudolinear chains of Te atoms. The band structure calculations show two steep bands arising from antibonding Te−Te interactions crossing the Fermi level parallel to *a**, pointing to one-dimensional metallic properties. The electrical conductivity and Seebeck coefficient measurements yielded values of around 180 $\Omega^{-1}\ cm^{-1}$ and 50 $\mu V\ K^{-1}$, respectively, at room temperature. The power factor was found to be 1.45 $\mu W\ cm^{-1}\ K^{-2}$ at 750 K, which is low compared to advanced thermoelectrics. This material could, on the other hand, become a useful thermoelectric, if large single crystals of defined orientation could be grown, but thus far our attempts to do so failed (or a Peierls distortion should be introduced).

ASSOCIATED CONTENT

Supporting Information

A crystallographic information file (CIF), two DSC/TG plots, and one COHP plot for the Cu−Te interactions of the model $Ba_2Cu_7Te_6$. This material is available free of charge via the Internet at http://pubs.acs.org.

AUTHOR INFORMATION

Corresponding Author

*E-mail: kleinke@uwaterloo.ca.

Notes

The authors declare no competing financial interest.

ACKNOWLEDGMENTS

Financial support from the Natural Sciences and Engineering Research Council is appreciated.

REFERENCES

(1) Kosbar, L. L.; Murray, C. E.; Copel, M.; Afzali, A.; Mitzi, D. B. *Nature* **2004**, *428*, 299−303.
(2) Tarascon, J.-M.; Armand, M. *Nature* **2001**, *414*, 359−367.
(3) Atwood, G. *Science* **2008**, *321*, 210−211.
(4) Lencer, D.; Salinga, M.; Grabowski, B.; Hickel, T.; Neugebauer, J.; Wuttig, M. *Nat. Mater.* **2008**, *7*, 972−977.
(5) Yamada, N.; Wuttig, M. *Nat. Mater.* **2007**, *6*, 824−832.
(6) Hsu, K. F.; Loo, S.; Guo, F.; Chen, W.; Dyck, J. S.; Uher, C.; Hogan, T.; Polychroniadis, E. K.; Kanatzidis, M. G. *Science* **2004**, *303*, 818−821.
(7) Chung, D.-Y.; Hogan, T. P.; Rocci-Lane, M.; Brazis, P.; Ireland, J. R.; Kannewurf, C. R.; Bastea, M.; Uher, C.; Kanatzidis, M. G. *J. Am. Chem. Soc.* **2004**, *126*, 6414−6428.
(8) Venkatasubramanian, R.; Slivola, E.; Colpitts, T.; O'Quinn, B. *Nature* **2001**, *413*, 597−602.
(9) Rowe, D. M. *Thermoelectrics Handbook: Macro to Nano*; CRC Press, Taylor & Francis Group: Boca Raton, FL, 2006.
(10) Toberer, E. S.; Cox, C. A.; Brown, S. R.; Ikeda, T.; May, A. F.; Kauzlarich, S. M.; Snyder, G. J. *Adv. Funct. Mater.* **2008**, *18*, 2795−2800.
(11) Toberer, E. S.; Brown, S. R.; Ikeda, T.; Kauzlarich, S. M.; Snyder, G. J. *Appl. Phys. Lett.* **2008**, *93*, 062110/1−062110/3.
(12) Xu, H.; Kleinke, K. M.; Holgate, T.; Zhang, H.; Su, Z.; Tritt, T. M.; Kleinke, H. *J. Appl. Phys.* **2009**, *105*, 053703/1−053703/5.
(13) Kleinke, H. *Chem. Mater.* **2010**, *22*, 604−611.

(14) Sootsman, J. R.; Kong, H.; Uher, C.; D'Angelo, J. J.; Wu, C.-I.; Hogan, T. P.; Caillat, T.; Kanatzidis, M. G. *Angew. Chem., Int. Ed.* **2008**, *47*, 8618−8622.
(15) Kanatzidis, M. G. *Chem. Mater.* **2010**, *22*, 648−659.
(16) Wang, Y. C.; DiSalvo, F. J. *J. Solid State Chem.* **2001**, *156*, 44−50.
(17) Patschke, R.; Zhang, X.; Singh, D.; Schindler, J.; Kannewurf, C. R.; Lowhorn, N.; Tritt, T.; Nolas, G. S.; Kanatzidis, M. G. *Chem. Mater.* **2001**, *13*, 613−621.
(18) Assoud, A.; Thomas, S.; Sutherland, B.; Zhang, H.; Tritt, T. M.; Kleinke, H. *Chem. Mater.* **2006**, *18*, 3866−3872.
(19) Cui, Y.; Assoud, A.; Xu, J.; Kleinke, H. *Inorg. Chem.* **2007**, *46*, 1215−1221.
(20) Mayasree, O.; Cui, Y. J.; Assoud, A.; Kleinke, H. *Inorg. Chem.* **2010**, *49*, 6518−6524.
(21) Mayasree, O.; Sankar, C. R.; Assoud, A.; Kleinke, H. *Inorg. Chem.* **2011**, *50*, 4580−4585.
(22) Mayasree, O.; Sankar, C. R.; Cui, Y.; Assoud, A.; Kleinke, H. *Eur. J. Inorg. Chem.* **2011**, 4037−4042.
(23) Kuropatwa, B.; Cui, Y.; Assoud, A.; Kleinke, H. *Chem. Mater.* **2009**, *21*, 88−93.
(24) Kuropatwa, B. A.; Assoud, A.; Kleinke, H. *Inorg. Chem.* **2011**, *50*, 7831−7837.
(25) Mayasree, O.; Sankar, C. R.; Kleinke, K. M.; Kleinke, H. *Coord. Chem. Rev.* **2012**, in press.
(26) Assoud, A.; Derakhshan, S.; Soheilnia, N.; Kleinke, H. *Chem. Mater.* **2004**, *16*, 4193−4198.
(27) Xu, J.; Kleinke, H. *J. Comput. Chem.* **2008**, *29*, 2134−2143.
(28) *M86-Exx078 APEX2 User Manual*; Bruker AXS Inc.: Madison, WI, 2006.
(29) Sheldrick, G. M. *Acta Crystallogr., Sect. A* **2008**, *64*, 112−122.
(30) Andersen, O. K. *Phys. Rev. B* **1975**, *12*, 3060−3083.
(31) Skriver, H. L. *The LMTO Method*; Springer: Berlin, Germany, 1984.
(32) Hedin, L.; Lundqvist, B. I. *J. Phys. C* **1971**, *4*, 2064−2083.
(33) Lambrecht, W. R. L.; Andersen, O. K. *Phys. Rev. B* **1986**, *34*, 2439−2449.
(34) Blöchl, P. E.; Jepsen, O.; Andersen, O. K. *Phys. Rev. B* **1994**, *49*, 16223−16233.
(35) Dronskowski, R.; Blöchl, P. E. *J. Phys. Chem.* **1993**, *97*, 8617−8624.
(36) Landrum, G. A.; Dronskowski, R. *Angew. Chem., Int. Ed.* **2000**, *39*, 1560−1585.
(37) Spangenberg, K. *Naturwissen* **1927**, *15*, 266−266.
(38) Li, J.; Guo, H.-Y.; Carey, J. R.; Mulley, S.; Proserpio, D. M.; Sironi, A. *Mater. Res. Bull.* **1994**, *29*, 1041−1048.
(39) Cordier, G.; Schwidetzky, C.; Schaefer, H. *Z. Naturforsch. B* **1984**, *39*, 833−834.
(40) Jansen, M. *Angew. Chem., Int. Ed.* **1987**, *26*, 1098−1110.
(41) Mehrotra, P. K.; Hoffmann, R. *Inorg. Chem.* **1978**, *17*, 2187−2189.
(42) Merz, K. M., Jr.; Hoffmann, R. *Inorg. Chem.* **1988**, *27*, 2120−2127.
(43) Pyykkö, P. *Chem. Rev.* **1997**, *97*, 597−636.
(44) Caillat, T.; Fleurial, J.-P.; Borshchevsky, A. *J. Phys. Chem. Solids* **1997**, *58*, 1119−1125.
(45) Snyder, G. J.; Christensen, M.; Nishibori, E.; Caillat, T.; Iversen, B. B. *Nat. Mater.* **2004**, *3*, 458−463.
(46) Schweika, W.; Hermann, R. P.; Prager, M.; Persson, J.; Keppens, V. *Phys. Rev. Lett.* **2007**, *2007*, 125501/1−125501/4.
(47) Batchelor, R. J.; Einstein, F. W. B.; Gay, I. D.; Jones, C. H. W.; Sharma, R. D. *Inorg. Chem.* **1993**, *32*, 4378−4383.
(48) Thiele, K.-H.; Steinicke, A.; Dümichen, U.; Neumüller, B. *Z. Anorg. Allg. Chem.* **1996**, *622*, 231−234.
(49) Canadell, E.; Jobic, S.; Brec, R.; Rouxel, J.; Whangbo, M.-H. *J. Solid State Chem.* **1992**, *99*, 189−199.
(50) Jepsen, O.; Andersen, O. K. *Z. Phys.* **1995**, *97*, 35−47.
(51) Peierls, R. E. *Quantum Theory of Solids*; Clarendon Press: Oxford, U.K., 1955.
(52) Choi, K.-S.; Kanatzidis, M. G. *J. Solid State Chem.* **2001**, *161*, 17−22.